

# Simulation Study of Granular Compaction Dynamics under Vertical Tapping

D. Arsenović<sup>1</sup>, S.B. Vrhovac<sup>1,a</sup>, Z.M. Jakšić<sup>1</sup>,  
Lj. Budinski-Petković<sup>2</sup> and A. Belić<sup>1</sup>

<sup>1</sup>Institute of Physics, P.O. Box 68, Zemun 11080, Belgrade, Serbia

<sup>2</sup>Faculty of Engineering, Trg D. Obradovića 6, Novi Sad 21000, Serbia

<sup>a</sup>vrhovac@phy.bg.ac.yu

**Keywords:** Granular compaction, Granular materials, Memory effects.

**Abstract.** We study by numerical simulation the compaction dynamics of frictional hard disks in two dimensions, subjected to vertical shaking. Shaking is modeled by a series of vertical expansions of the disk packing, followed by dynamical recompression of the assembly under the action of gravity. The second phase of the shake cycle is based on an efficient event-driven molecular-dynamics algorithm. We analyze the compaction dynamics for various values of friction coefficient and coefficient of normal restitution. We find that the time evolution of the density is described by  $\rho(t) = \rho_\infty - \Delta\rho E_\alpha[-(t/\tau)^\alpha]$ , where  $E_\alpha$  denotes the Mittag-Leffler function of order  $0 < \alpha < 1$ . The parameter  $\tau$  is found to decay with tapping intensity  $\Gamma$  according to a power law  $\tau \propto \Gamma^{-\gamma}$ , where parameter  $\gamma$  is almost independent of the material properties of grains. Also, an expression for the grain mobility during compaction process has been obtained.

## Introduction

The phenomenon of granular compaction involves the increase of the density of granular material subjected to shaking, tapping or, more generally, to some kind of external excitation. The underlying dynamic and structural properties of compaction process have been a subject of great interest for physicists in recent years [1-5].

A main difficulty in studying compaction is that tapping experiments involve two different series of elementary processes of quite different nature, and realistic models for both of these processes are needed. In the first process, mechanical energy is supplied to a powder in the form of external excitation, and free volume is introduced instantaneously throughout the system. Excitations are followed by the periods of release during which the grains and voids have some freedom to rearrange their positions relative to their neighbors. The waiting time between successive taps is long enough to allow the system to relax, so that the initial state for each tap is the final state from the previous relaxation. The consecutive repetition of both processes, tapping and free evolution, reduces the porosity of the material and makes it denser.

The modeling of both processes, tapping and free evolution, is a rather difficult task, although some procedures have been proposed. Our numerical simulation is based on the ideas of Barker and Mehta [6,7] and Bideau and coworkers [8], with modifications aiming at more realistic treatment of gravitational redeposition of granular particles.

Our simulations have been performed for a two-dimensional system of frictional monosized hard disks in the rectangular geometry. During the redeposition of the packing, the disks undergo instantaneous, inelastic binary collisions and propagate under gravity in between collision events. Their settlement is terminated when the total kinetic energy of each disk falls below some threshold value. Previously observed multi-particle structures (arches or bridges) [7, 9] are seen to naturally emerge in the simulation. The algorithm employed in the present paper describes relatively accurately the quite complex succession of collisions in a shaken packing and provides realistic information about its microstructural transformations during compaction.

### Simulation method

In the simulation, the compaction of  $N=1000$  monosize disks of diameter  $d$  and mass  $m$  under consecutive taps is studied in a rectangular container of width  $L=1$ , with a flat bottom at  $y=0$  and opened top. A gravitational field  $\vec{g}$  acts downwards, i.e., along the negative  $y$  direction. One shake cycle of the granular assembly (corresponding to one time step of our simulation) is decomposed in two stages: 1) vertical dilatation of the disk packing, in proportion to the shaking acceleration  $\Gamma$  and 2) formation of static granular pack in the presence of gravity. Repeated application of the shaking algorithm builds a sequence of static packings where each new packing is built from its predecessor.

In the first phase of the shake cycle, free volume is introduced uniformly throughout the whole packing. A disk at height  $y$  is raised to a new height  $y'=(1+\xi)y$ . This models the dilation phase of a vibrated granular medium. In that sense, the parameter  $\xi$  in our model plays a similar role as  $\Gamma$  in real experiments. The latter is defined as the ratio of the peak acceleration of the tap to the gravitational acceleration [1].

After dilation, we give a random initial velocity to each disk, in such a way that the total momentum is equal to zero. In the second phase of the shake cycle, the packing is compressed under gravity, using an efficient event-driven molecular-dynamics algorithm [10]. The disks are assumed to be inelastic with rough surfaces subject to Coulomb friction. In the event driven method the disks follow an undisturbed motion, under the influence of gravity, until an event occurs. An event is either the collision of two disks or the collision of one disk with the wall. Particle collisions are modeled using the Walton model [11,12]. This model implies that two disks at contact either slide, following Coulomb's law, or stick together. The collision rule takes into account a reduction of normal relative velocity of the two particles and a reduction of total tangential relative velocity. To prevent an inelastic collapse [13-15], we use a coefficient of restitution which depends on the relative colliding velocity of the particles.

Due to dissipative collisions, the potential energy of the system tends towards a constant, while its kinetic energy tends towards zero in the long time limit. A static configuration of disks with zero kinetic energy is reached by imposing the following stopping criteria. A disk is considered to be at rest if both translational and rotational kinetic energy of the disk in the last ten collisions falls below a threshold value  $E_{tr}^{(t)}$  and  $E_{tr}^{(r)}$ , respectively. In this study, we used very low values  $E_{tr}^{(t)} = 5 \times 10^{-5}$  and  $E_{tr}^{(r)} = 10^{-6}$ , in dimensionless units based on disk mass  $m$ , container width  $L$ , and arbitrary time unit  $T$ .

These simulations were performed on parallel cluster computer consisting of 100 Intel processors. A typical simulation of entire compaction process used 3 CPU days on a single processor.

### Results and Discussion

In order to examine the effects of inelastic and friction properties of grains on compaction dynamics we used two sets of material parameters. More dissipative and rough disks (referred hereafter as disks (A)) are characterized by coefficients of inelasticity  $\varepsilon_0=0.6$  and friction coefficient  $\mu=0.4$ , whereas with parameters  $\varepsilon_0=0.9$  and  $\mu=0.2$  we characterize less dissipative disks (disks (B)). We used the same inelasticity and friction coefficients for grain-grain and grain-wall collisions including the horizontal base.

The variation of the packing fraction  $\rho(t)$  with the number of shakes  $t$  for several tapping intensities  $\xi$  is presented in Fig. 1, where more dissipative grains (disks (A)) have been used. The inset of Fig. 1 compares the evolution of normalized packing fraction  $\tilde{\rho}(t) = (\rho(t) - \rho(0)) / (\rho(\infty) - \rho(0))$  for two kinds of grains (A) and (B), for  $\xi=3\%$ . The simulation curves are in good qualitative agreement with the data obtained in experiments with a reduced lateral confinement [2,3].

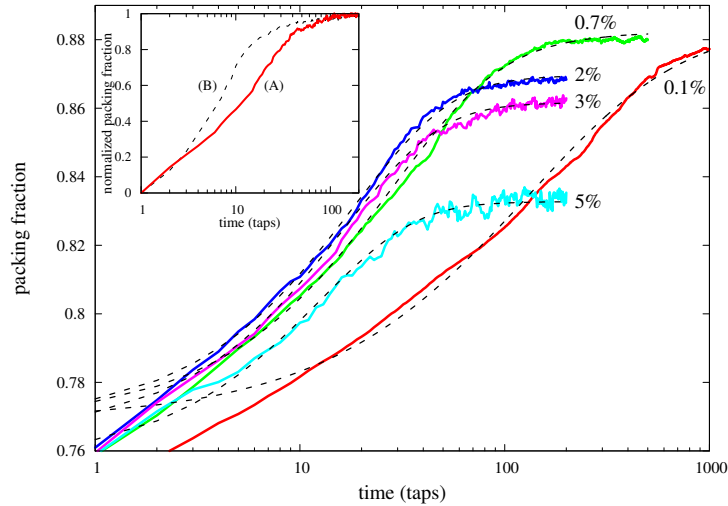


Fig. 1 (Color online) Temporal evolution of the packing fraction  $\rho(t)$  obtained for the grains of type (A) and for various tapping intensities  $\xi = 0.1\%$  (red),  $0.7\%$  (green),  $2\%$  (blue),  $3\%$  (violet) and  $5\%$  (light blue). The dashed curves are the Mittag–Leffler fits of Eq. (1), with the parameters  $\tau$  and  $\alpha$  given in Fig. 2. Inset: evolution of the normalized packing fraction for two kinds of grains (disks (A) – solid line and disks (B) – dashed line), at  $\xi = 3\%$ .

We have observed that compaction dynamics gets slower when tapping intensity  $\xi$  decreases. Actually, when a small tapping intensity is applied the evolution of the density toward steady–state value  $\rho_\infty$  takes place on a much wider time scale and finally a higher value of the asymptotic packing fraction is achieved.

Recently, we carried out extensive simulations of reversible random sequential adsorption (RSA) using objects of different sizes and rotational symmetries on a triangular lattice [16]. This lattice–based model can be regarded as a simple model for the compaction of granular objects of various shapes. Note that the ratio of desorption/adsorption probability ( $1/K=P_-/P_+$ ) plays in the reversible RSA model a role similar to the intensity of vibration  $\Gamma$  in real experiments. We showed [16] that the resulting compaction dynamics is strongly consistent with the Mittag–Leffler law

$$\rho(t) = \rho_\infty - \Delta\rho E_\alpha[-(t/\tau)^\alpha], \quad \Delta\rho = \rho_\infty - \rho_0 \quad (1)$$

Here  $\rho_0$  is the initial packing fraction and  $\rho_\infty$  is the mean value of the packing fraction at the stationary state.  $E_\alpha$  denotes the Mittag–Leffler function of order  $\alpha$ . Our data are reasonably well fitted by a Mittag–Leffler function (1). These fits are shown by dashed lines in Fig. 1. As can be seen, the intermediate–long time behavior of the packing fraction can be accurately described by Eq. (1).

In Fig. 2 the values of two fitting parameters  $\tau$  and  $\alpha$  versus control parameter  $\xi$  are reported for the both kinds of grains, (A) and (B). The parameter  $\tau$ , for a given type of grains, seems to be a simple power law of the vibration intensity  $\xi^{1/2} \propto \Gamma$ :

$$\tau = K \xi^{-\gamma/2}. \quad (2)$$

As one can see from Fig. 2, the slope of  $\tau$  vs  $\xi^{1/2}$  curves is almost independent of the material properties of the grains. For disks of type (A) and (B) the exponents are  $\gamma^{(A)}=2.50$  and  $\gamma^{(B)}=2.85$ , respectively.

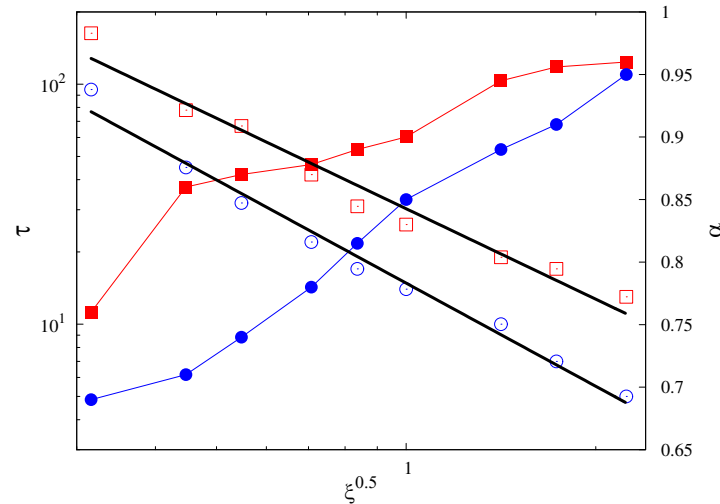


Fig. 2 Fit parameters  $\tau$  (empty symbols) and  $\alpha$  (full symbols) of (1), as functions of vibration intensity  $\xi^{1/2} \propto \Gamma$  for two kinds of grains. Squares and circles correspond to the grains of type (A) and (B), respectively. The straight lines are fits using Eq. (2).  $\tau(\Gamma)$  seems to be well described by simple power law.

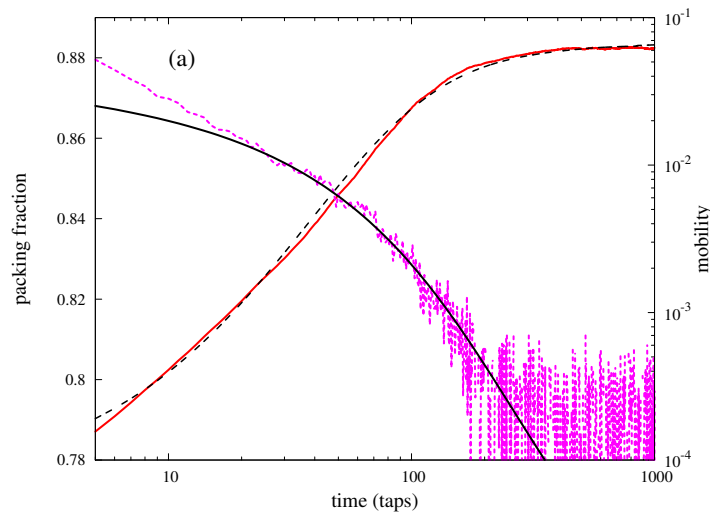


Fig. 3 (Color online) Simulation results for time behavior of the mobility  $\mu(t)$  (dotted line) and density  $\rho(t)$  (red solid line) for excitation parameter  $\xi = 0.5\%$ . These results come from an average over 80 simulations. Parameter  $k$  from Eq. (5) is 0.94. The dashed superimposed line is a fit according to Eq. (1). The black solid curve is mobility  $\mu(t)$  calculated from Eq. (5).

However, the parameter  $K$  of the power law (2) depends appreciably on the material properties of the grains. We have obtained that  $K^{(A)}=30.3$  and  $K^{(B)}=13.1$  for disks (A) and (B), respectively. This kind of power-law dependence of the parameter  $\tau$  was also observed in the Mittag-Leffler fits (1) of the coverage fraction in lattice based reversible RSA model [16].

One striking feature of Fig. 2 is the fact that the fitting parameter  $\alpha$  depends considerably on the tapping intensity  $\xi^{1/2} \propto \Gamma$  and on the material properties of the grains. For high values of  $\xi^{1/2}$ , there is a rapid approach to steady-state density  $\rho_\infty$ , and consequently the parameter  $\alpha$  reaches a value close to 1. Since  $E_\alpha[-(t/\tau)^\alpha] \rightarrow \exp(-t/\tau)$  when  $\alpha \rightarrow 1$ , the slow ('glassy') relaxation feature disappears in the regime of strong tapping intensities.

The steady-state density  $\rho_\infty$  is also sensitive to the material properties of disks. The decrease of  $\rho_\infty$  with  $\xi^{1/2}$  is more pronounced for disks of type (A). However, for the given tapping intensity, the system of disks (B) achieves a higher value of the asymptotic density  $\rho_\infty$  than the system of more dissipative disks (A).

The next stage consists of studying the relationship between compaction dynamics and mobility of the grains. In this study we work with the following definition of the grain mobility:

$$\mu(t) = -\frac{1}{N} \sum_{i=1}^N \frac{\langle y_i(t+1) - y_i(t) \rangle}{d}, \quad (3)$$

where  $N$  is the number of particles,  $y_i(t)$  is the  $y$ -coordinate of the  $i$ th particle at time  $t$  and the angular brackets denote an average over independent runs. Here, time is measured in such a way that unity corresponds to one tap. When compaction goes on, the grain mobility decreases. We expect that the mobility vanishes when the packing fraction  $\rho$  becomes close to its asymptotic or steady-state limit  $\rho_\infty$ . Hence, the variation of the normalized packing fraction induced by a tap should be proportional to mobility  $\mu$ ,

$$\frac{\partial \tilde{\rho}}{\partial t} = k\mu, \quad (4)$$

where  $k$  is a constant.

Substituting Eq. (1) into Eq. (4) we obtain an analytical expression for  $\mu$ ,

$$\mu(t) = -\frac{1}{k} \frac{1}{t} E_{\alpha,0} \left( -\left(\frac{t}{\tau}\right)^\alpha \right). \quad (5)$$

Here  $E_{\alpha,\beta}$  is generalized Mittag-Leffler function [17].

We have checked Eq. (5) by comparing it with the results obtained from the numerical simulation. An example is given in Fig. 3 where we have plotted both mobility  $\mu(t)$  and density  $\rho(t)$  as functions of the number of taps  $t$ . The data shown have been obtained in a system composed of the grains of type (A), and have been averaged over 80 runs. In the same figure the fits to the Mittag-Leffler law Eq. (1) are also given, demonstrating that it is excellently obeyed. The two fitting parameters are  $\tau = 42.2$ ,  $\alpha = 0.878$  for  $\xi = 0.5\%$ . The superimposed continuous curve in Fig. 3 is the mobility calculated from Eq. (5) by using the above quoted fitting parameters. As can be seen, in all cases the functional form (5) is quite well satisfied for times beyond initial stage of relaxation process.

It is interesting to note that the fitting function (1) is a solution of the fractional kinetic equation [18]:

$$\frac{d}{dt} \Delta\rho(t) = -\tau^\alpha {}_0D_t^{1-\alpha} \Delta\rho(t), \quad 0 < \alpha < 1, \quad (6)$$

where  $\Delta\rho(t) = \rho_\infty - \rho(t)$ . Operator  ${}_0D_t^{1-\alpha}$  is the Riemann-Liouville (R-L) operator of fractional integration:

$${}_0D_t^{1-\alpha} \Delta\rho(t) = \frac{1}{\Gamma(\alpha-1)} \int_0^t (t-t')^{\alpha-2} \Delta\rho(t') dt' \quad (7)$$

The R-L operator introduces a convolution integral into Eq. (6) with the power-law kernel  $M(t) \propto t^{\alpha-2}$ . Therefore, the fractional kinetic equation (6) involves a slowly decaying memory, so the present density  $\rho(t)$  of the system depends strongly on its history  $\rho(t')$ ,  $t' < t$ . This is in accordance with the fact that granular materials are intrinsically non-local.

## Conclusion

We have demonstrated that large scale simulations of granular compaction offer insight into dynamics of the compaction process and evolution of the packing structure during its progressive densification. Unlike almost all previous models for granular compaction, whose essential ingredient is geometrical frustration, our model is based on realistic granular dynamics. One of its main features is that during the second phase of the shake cycle the whole system is reassembled by using event-driven molecular-dynamics algorithm. We employed the Walton model [11,12] that captures the major features of granular interactions.

We have fitted the time dependences of the packing fraction with the Mittag-Leffler function (1). Our data show that the compaction dynamics strongly depends on the material properties of the grains. It was shown that the relaxation behavior is appreciably slowing down with the increase of the inelasticity of the grains. The characteristic timescale  $\tau$  is found to decay with tapping intensity  $\Gamma$  according to a power law (2),  $\tau \propto \Gamma^{-\gamma}$ . The exponent  $\gamma$  is almost independent of the material properties of the grains. However, it is not clear whether Eq. (1) is just a convenient fitting expression with four parameters or it has a more fundamental meaning, associated to some peculiar dynamical events, which are dominant in the relaxation of the density. We hope to elucidate this point more thoroughly in a future work in order to develop a fractional model of granular compaction that captures this relaxation dynamics.

In order to study the dynamics of compaction, we have also analyzed the mobility of the grains. We have proposed an analytical expression (5) for mobility which is consistent with simulation data. Finally, the model presented here can be easily generalized to mixtures of several kinds of grains, allowing the study of segregation phenomena.

## Acknowledgement

This research was supported by the Ministry of Science and Environmental Protection of the Republic of Serbia, under Grants No. 141035 and No. 141003.

## References

- [1] J.B. Knight, C.G. Fandrich, C.N. Lau, H.M. Jaeger and S.R. Nagel: Phys. Rev. E Vol. 51, (1995), p. 3957.
- [2] P. Philippe and D. Bideau: Europhys. Lett. Vol. 60 (2002), p. 677.
- [3] P. Ribière, P. Richard, D. Bideau and R. Delannay: Eur. Phys. J. E Vol. 16 (2005), p. 415.
- [4] G. Lumay and N. Vandewalle: Phys. Rev. Lett. Vol. 95 (2005), p. 028002.
- [5] M.J. de Oliveira and A. Petri: J. Phys. A: Math. Gen. Vol. 31 (1998), p. L425.
- [6] G.C. Barker and A. Mehta: Phys. Rev. A Vol. 45 (1992), p. 3435.
- [7] A. Mehta, G.C. Barker and J.M. Luck: J. Stat. Mech.: Theor. Exp. October (2004), P10014.
- [8] P. Philippe and D. Bideau: Phys. Rev. E Vol. 63 (2001), p. 051304.
- [9] A. Ferguson and B. Chakraborty: Phys. Rev. E Vol. 73 (2006), p. 011303.
- [10] D. Lubachevsky: J. Comp. Phys. Vol. 94 (1991), p. 255.
- [11] O.R. Walton and R.L. Braun: J. Rheology Vol. 30 (1986), p. 949.
- [12] O. Herbst, M. Huthmann and A. Zippelius: Granular Matter Vol. 2 (2000), p. 211.
- [13] D. Goldman, M.D. Shattuck, C. Bizon, W.D. McCormick, J.B. Swift and H.L. Swinney: Phys. Rev. E Vol. 57 (1998), p. 4831.
- [14] E. Falcon, C. Laroche, S. Fauve and C. Coste: Eur. Phys. J. B Vol. 3 (1998), p. 45.
- [15] S. McNamara and E. Falcon: Phys. Rev. E Vol. 71 (2005), p. 031302.
- [16] Lj. Budinski-Petković, M. Petković, Z.M. Jakšić and S.B. Vrhovac: Phys. Rev. E Vol. 72 (2005). P. 046118.
- [17] K.S. Miller and B. Ross: *An introduction to the fractional calculus and fractional differential equation* (A Wiley-Interscience Publication 1993).
- [18] R.K. Saxena, A.M. Mathai and H.J. Haubold: Physica A Vol. 344 (2004), p. 657.